

INFLUENCE OF SUBSTRATE LOADING AND DETACHMENT CONDITIONS ON A PLANE BIOFILM BEHAVIOUR

Michał Blatkiewicz¹, Bolesław Tabiś², Stanisław Ledakowicz^{1*}

¹Lodz University of Technology, Faculty of Process and Environmental Engineering,
ul. Wólczajska 213, 90-942, Łódź, Poland

²Cracow University of Technology, Faculty of Chemical Engineering and Technology,
ul. Warszawska 24, 31-155 Kraków, Poland

A mathematical model of a plane, steady state biofilm, with the use of a single substrate kinetics, was proposed. A set of differential equations was solved. In order to analyse the biofilm's behaviour, a number of simulations were performed. The simulations included varying process parameters such as detachment coefficient and substrate loading. Two detachment models were taken into consideration: one describing the detachment ratio as proportional to the thickness of the biofilm, and the other one proportional to the thickness of the biofilm squared. The results provided information about substrate and live cell distribution in biofilm and the influence of certain parameters on biofilm behaviour.

Keywords: biofilm, modeling, growth kinetics

1. INTRODUCTION

In nature, microorganisms occur in various forms. They can exist in a free form, as a single specimen, when they are referred to as planktonic microorganisms. They can also attract each other, forming pairs and colonies. Beside these states, it was proven that many species of microorganisms have the ability to adhere to solid surfaces, forming continuous layers called biofilms.

A biofilm can be described as a multicellular structure made of microorganisms growing on a surface of a solid structure with access to water. It can be found on almost any surface where the environment is propitious for microorganisms. Biofilms can develop on both natural vessels and those created artificially. Plaque, deposits on water tanks' facets or layers on plant surfaces, are examples of naturally grown biofilms. Depending on the microorganisms that the biofilm consists of, it can occur in environments normally unfit to sustain life, such as ocean bottoms, hot springs or arctic rocks (Stewart et al., 1996).

Investigation of biofilms is not pursued solely by its technological purposes. It is estimated that around 80% of bacterial infections is caused not by planktonic microorganisms, but by bacteria in the immobilised state of biofilm (Janssens et al., 2008). Due to the fact that in such a state, microorganisms are much more robust and immune to antibiotics (Sidhu et al., 2001), biofilm disinfection is an important and widely researched issue, especially in the food industry, to prevent foodborne disease outbreaks (Srey et al., 2012).

*Corresponding author, e-mail: stanleda@p.lodz.pl

Biofilms can be divided into two basic groups. The first type is a monolayer, in which the specimens can adhere only to the surface, making the biofilm only one cell thick. The other type is a multilayer film which can grow large enough to be seen by the naked eye. Its growth and metabolism are much more complicated than in the case of a monolayer, and the potential technological application is much wider (Topiwala and Hamer, 1971). This article focuses only on multilayer biofilms.

The formation and life cycle of a biofilm is a complicated phenomenon. First, specimens adhere to the surface with the van der Waals force, and often are able to prevent disconnection by anchoring themselves using, for example, insets. After having created the initial structure, the cells start to produce chemical compounds that build a matrix, which connects them into a continuous texture. The matrix not only keeps the cells together, but also makes it more resistant to external factors and, in advanced structures, can even turn the biofilm into an advanced pseudo-organism. Eventually, the cells on the border of the biofilm can separate themselves from the structure and enter the liquid phase. This is the self-acting part of the biofilm detachment (Stoodley et al., 2002).

Various parameters are used to define the physical structure of a biofilm, such as its density, porosity, surface area or roughness. It was observed that these parameters can vary in a very wide range, depending on external factors like compression or tensile force (Laspidou and Aravas, 2007). Also, shear stress applied to the surface of a biofilm was proven to significantly affect the detachment of biofilm, especially the outer layers, which have smaller density and larger porosity (Paul et al., 2012).

The detachment of biofilm is one of the most complicated issues concerning biofilm modeling, and it is still difficult to create a satisfactory mathematical model that would include all the factors affecting it. According to Bryers (1988), the most important factors that should be considered while modelling biofilm detachment are erosion, sloughing, abrasion, grazing, and human intervention. The most basic and common factors are erosion and sloughing. Both are self-acting mechanisms of biofilm, which result in microorganisms being released from the immobilised structure to planktonic form. The difference between them is that while erosion is considered continuous, sloughing is considered discontinuous and stochastic. Abrasion occurs when two or more vessels of the biofilm collide, causing the structure to rub off the surface, which is a common issue in Biofilm Airlift Suspension (BAS) reactors. Grazing is caused by predatory organisms, and human intervention should be understood by removing the biofilm from the surface using mechanical methods (Kommedal and Bakke, 2003).

The importance of the described factors is diverse depending on the specified problem, making it very difficult to create a universal model of biofilm detachment. In this paper, the detachment is considered continuous, described by first or second order kinetics.

Mathematical modelling of biofilms can be performed using many different approaches. Because the usually considered vessels on which biofilms grow are planar or their curvature can be neglected, planar models are the most common. However, cylindrical and granular models for different vessels have also been considered (Liu and Horn, 2011).

Although the structure of a biofilm can often be simplified to smooth and uniform, two-dimensional models are also being developed to simulate changes in its surface and interior structure under specific conditions, an example of which is the model presented by Liao et al. (2012).

The majority of mathematical models of biofilms are based on two-substrate kinetics, of which one concerns the carbon source substrate, while the other - oxygen. In the presented work a single substrate kinetics model was taken into consideration. Such models can be applied not only to anaerobic processes, but also to those in which oxygen can be considered as being sufficiently supplied (Hsien and Lin, 2005)

The reason to create the mathematical model presented in this paper was to determine the influence of process parameters included in the model on its composition and thickness and to investigate substrate,

live cell and growth rate distributions within the biofilm. The simulations featured in the further parts of this paper concern one-substrate processes with the use of Monod kinetics, but the mathematical model can be extended to multi-substrate kinetics.

2. MODELLING

According to Wanner and Gujer (1985), the microbial composition of a biofilm is determined mostly by three factors: diffusional transport of substrates within its structure, microbial conversion of the substrates and biomass expansion. The presented model was built on the same principles.

The assumptions of the model included several simplifications, due to the fact that the chosen mechanisms were considered accurate enough for the model to be precise. In the model the biofilm was regarded as being in a steady state, because the dynamics of its behaviour was not the goal in this work, also because the dynamics of a biofilm highly depends on the structure's complete history, which makes it more difficult to create a working dynamic model (Wanner and Gujer, 1985). Since the thickness of a biofilm is usually very small compared to that of the liquid phase, it was assumed for calculation purposes that the concentrations of the carbon source substrate and dispersed microorganisms in the liquid phase could be assumed constant. There was no necessity to simulate the shape of the biofilm surface. Therefore, the biofilm was treated as a plane object, the composition of which changes only in the direction perpendicular to its base, thus making the model one-dimensional. It was assumed that the total density of cells was constant in the whole volume of the biofilm, and also that the densities of live and dead cells added up to a constant value. Neither oxygen transfer, predatory organisms, nor biofilm growth inhibitors like antibiotics were taken into consideration

Figure 1 shows a schematic drawing of a segment of biofilm considered in the model.

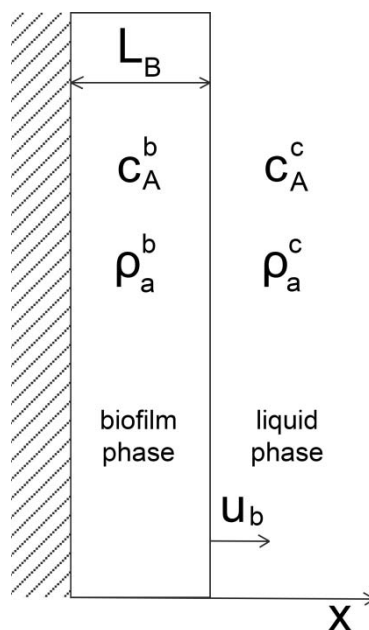


Fig. 1. Schematic drawing of a fragment of biofilm

The model consists of a set of differential equations with suitable boundary conditions. The processes considered include transport of dissolved ingredients to the surface of biofilm, use of the substrate by the immobilised microorganisms according to the considered model of metabolism, proliferation of the bacteria, movement of the cells inside the biofilm, death of the microorganisms and biofilm

detachment. The model principles are similar to those presented by Stewart et al. (1996), although the former included neither changing concentrations in the liquid phase nor the use of biocides.

The processes and corresponding mechanisms considered in the presented model are listed in the Table 1.

Table 1. Assumptions of the model

Liquid phase behavior	Like for completely stirred reactor; concentrations constant
Transport of dissolved ingredients within the biofilm	Fick's law of diffusion through inert component
External mass transfer	Convective mass transfer
Use of substrate	Proportional to biomass growth by the yield coefficient
Growth of biomass	Monod's model
Death of microorganisms	First order death rate
Transport of cells	Advection related to biomass growth
Biofilm detachment	a) Model proportional to biofilm thickness b) Model proportional to biofilm thickness squared

A dimensionless linear variable z was introduced:

$$z = \frac{x}{L_b} \quad (1)$$

A set of differential equations was proposed:

$$\frac{d^2 c_A^b}{dz^2} = \frac{\rho_a^b}{D_{eA} w_{BA}} \frac{\mu_{\max} c_A^b}{K_S + c_A^b} L_b^2 \quad (2)$$

$$\frac{d\rho_a^b}{dz} = \frac{1}{u_b} \left(1 - \frac{\rho_a^b}{\rho_b^b} \right) \frac{\mu_{\max} c_A^b}{K_S + c_A^b} \rho_a^b L_b - \frac{k_o}{u_b} \rho_a^b L_b \quad (3)$$

$$\frac{du_b}{dz} = \frac{\rho_a^b}{\rho_b^b} \frac{\mu_{\max} c_A^b}{K_S + c_A^b} L_b \quad (4)$$

and the fourth algebraic equation:

$$u_b(1) = k_{\det} f(L_b) \quad (5)$$

where

$$f(L_b) = L_b \quad \text{or} \quad f(L_b) = L_b^2 \quad (6)$$

The boundary conditions were the following:

$$\frac{dc_A^b(0)}{dz} = 0 \quad (7)$$

$$D_{eA} \frac{dc_A^b(L_b)}{dz} = k_s [c_A^c - c_{As}] L_b \quad (8)$$

$$u_b(0) = 0 \quad (9)$$

$$\rho_a^b(0) = \left[1 - \frac{k_o (K_S + c_A^b(0))}{\mu_{\max} c_A^b(0)} \right] \rho_b^b \quad (10)$$

where the condition (10) was formulated from the Equation (3) with the use of the condition (9).

Since the presented set of differential equations cannot to be solved analytically, numerical methods had to be used. The integration of the equations was performed using the Runge-Kutta method, and to correct the initial values, the Newton method was used. The initial step was to assume the values of substrate concentration at the base of the biofilm ($c_A^b(0)$) and the thickness of the biofilm (L_b). Then, the set of equations was solved, and the results compared to values given by the boundary conditions. If the results were incorrect, the initial values were fixed with the use of the Newton's method, and the set of equations was solved again until the results were correct.

3. RESULTS AND DISCUSSION

With the use of the proposed mathematical model and the designed program for numerical calculations, a few sets of simulations were performed. Due to lack of experimental data to perform calculations, the model parameters were taken from the literature (Stewart et al., 1996), in which the kinetic diffusion coefficient for the biofilm was considered equal to its equivalent for the liquid phase, and the mass penetration coefficient was given an exemplary value.

The values of the model parameters were listed in Table 2. The main purpose was to compare two of the biofilm detachment models (Kommedal and Bakke, 2003), of which one of the detachment rates was proportional to biofilm thickness (Peyton and Characklis, 1992), and the other one was proportional to biofilm thickness squared (Stewart et al., 1996).

Table 2. List of the parameters used in the model (Stewart et al., 1996)

ρ_b	30 [kg/m ³]
D_e	$2.375 \cdot 10^{-5}$ [m ² /h]
w_{BA}	0.45 [kgB/kgA]
μ_{\max}	0.3125 [1/h]
K_S	$2.550 \cdot 10^{-3}$ [kg/m ³]
k_o	$4.167 \cdot 10^{-4}$ [1/h]
k_s	0.02 [m/h]

3.1. Analysis of steady state solutions

The results of the simulations were presented to illustrate distributions of carbon substrate, active cells and biofilm growth as functions of dimensionless variable perpendicular to the biofilm's base. The assumed values of the biofilm detachment rate coefficients were picked in a way which would provide possibly analogous conditions. Therefore, for the first case, in which $r_{det1} = k_{det} L_b$, the detachment coefficient was equal $k_{det} = 0.1$ [1/h], and for $r_{det2} = k_{det} L_b^2$, the detachment coefficient was equal

$k_{det} = 100 [1/mh]$. In both cases the concentration of carbon substrate in the liquid phase was $c_A^C = 0.08 [kg/m^3]$.

Fig. 2 and Fig. 3 show respectively the carbon substrate distribution for r_{det1} and r_{det2} . A significant difference can be observed. While in the first case the curve is regular, for the detachment rate proportional to biofilm thickness squared, the values of substrate concentration in the biofilm drop to nearly zero in about half of the biofilm thickness - this outcome suggests that about half of the specimens in the biofilm have very limited access to carbon substrate. This phenomenon can be explained by the results shown in Figures 4 and 5, where for the r_{det2} the concentrations of active cells in the area near the interface are higher than those in the case of r_{det1} kinetics. In the first case, the thickness was equal to $L_{b1} = 5.56 \cdot 10^{-4} m$, and in the second case it was significantly lower, with the value of $L_{b2} = 3.10 \cdot 10^{-4} m$. These results suggest that the model of detachment proportional to squared biofilm thickness shows biofilms of lower thickness.

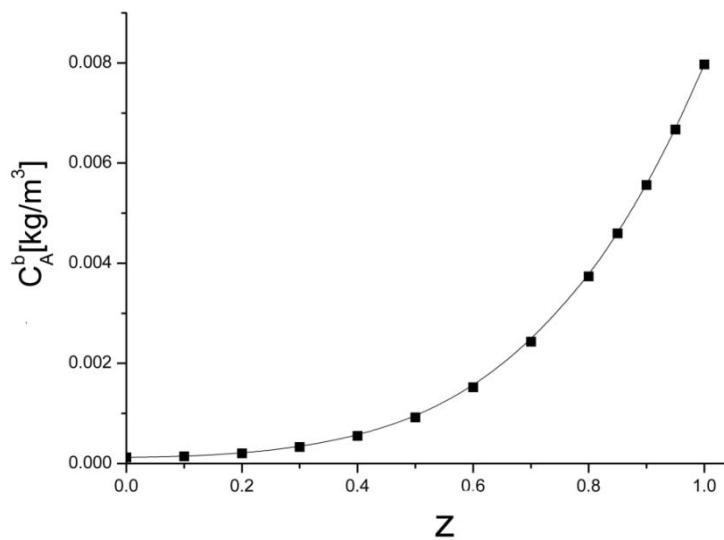


Fig. 2. Distribution of substrate concentration in biofilm as a function of dimensionless variable z with r_{det1} detachment kinetics

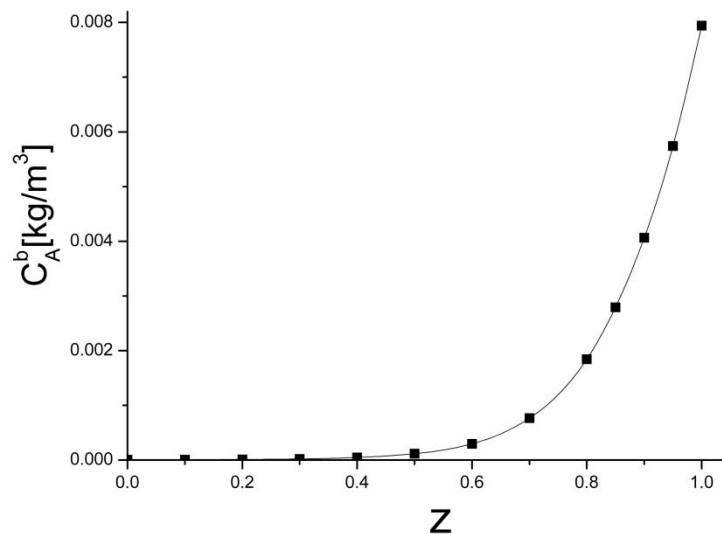


Fig. 3. Distribution of substrate concentration in biofilm as a function of dimensionless variable z with r_{det2} detachment kinetics

Figures 4 and 5 present distributions of active cells within the biofilm analogously to the situation with Figures 1 and 2. A big difference in the results was observed. While in the case of $r_{det} = r_{det1}$ the concentration of live cells was almost constant (difference less than 3%), in the case of $r_{det} = r_{det2}$, the concentration of active cells at the biofilm base fell by over 60% of the value on the edge of the biofilm. The biggest drop in the concentration of live cells starts at the point where the values of substrate concentration are very low.

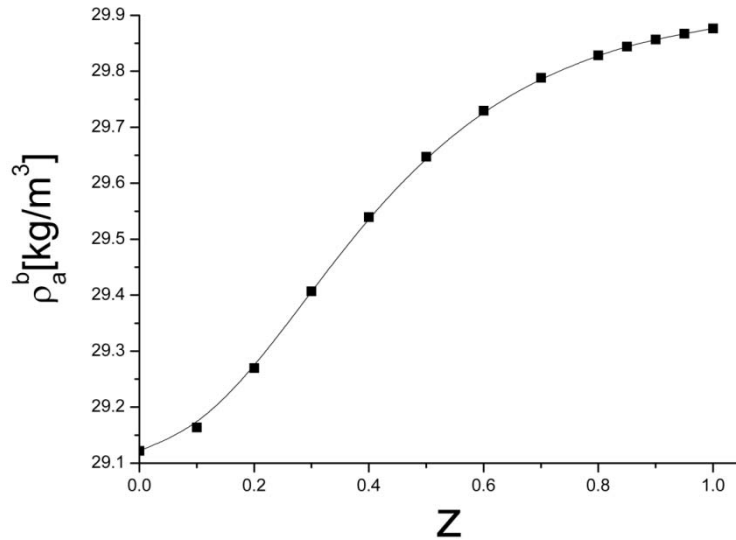


Fig. 4. Distribution of live cells concentration in biofilm as a function of dimensionless variable z with r_{det1} detachment kinetics

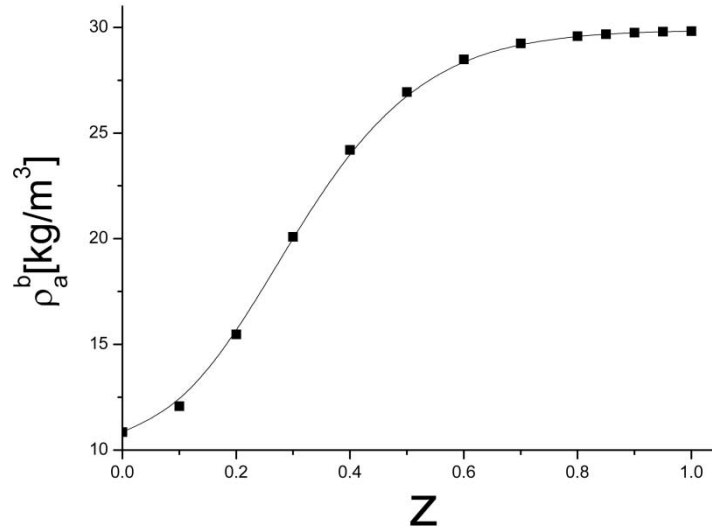


Fig. 5. Distribution of live cells concentration in biofilm as a function of dimensionless variable z with r_{det2} detachment kinetics

The curves representing the rate of biofilm growth as a function of the dimensionless variable z , shown in Figures 6 and 7 have shapes similar to their corresponding distributions of substrate. It can be noticed then that access to the substrate determines the rate of biofilm growth, which also can be concluded from the Equation (3). It is also important to notice that, regardless of assumed detachment model, therefore the biofilm thickness as well, the biofilm growth rates at the edge of the biofilm are almost identical, corresponding to the concentration of substrate on the edge of biofilm.

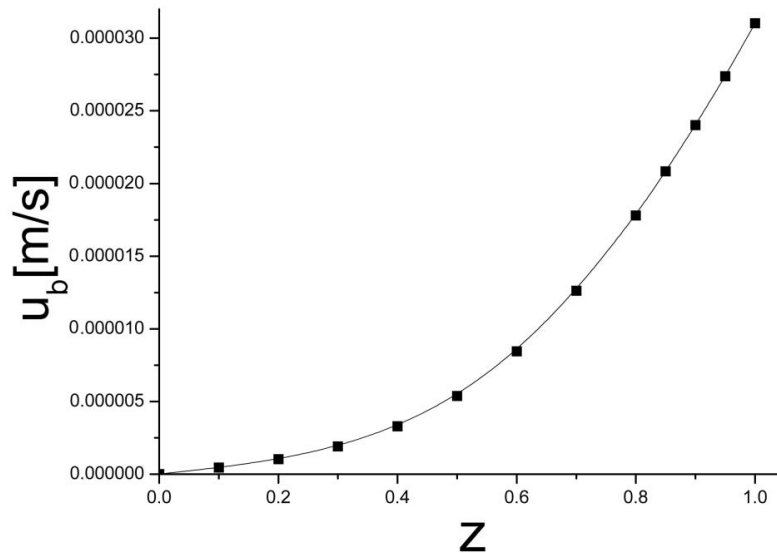


Fig. 6. Biofilm growth rate as a function of dimensionless variable z with r_{det1} detachment kinetics

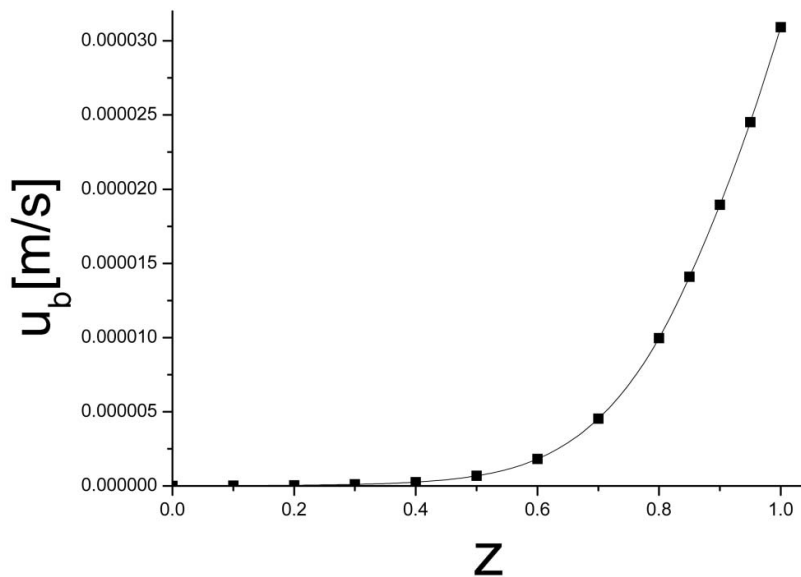


Fig. 7. Biofilm growth rate as a function of dimensionless variable z with r_{det2} detachment kinetics

3.2. Analysis of results for varying substrate concentration and detachment coefficient

The numeric simulations can be divided into two basic groups, depending on the assumed detachment models. Specific values in characteristic areas were taken into consideration, including concentration of substrate at the base of biofilm, concentration of live cells at the base of biofilm and rate of biofilm growth at the edge of biofilm. Neither the concentrations of substrate and live cells at the edge of biofilm nor the rate of biofilm growth at the base of biofilm were compared, because their values were determined directly by the boundary conditions. Additionally, the biofilm thickness values received with the use of the aforementioned simulations were presented. In all cases the values of liquid phase substrate concentrations were equal to $c_A^c = \{0.06, 0.07, 0.08, 0.09, 0.1\} [\text{kg}/\text{m}^3]$. For $r_{det} = r_{det1}$ the values of the detachment coefficient were equal to $k_{det} = \{0.06, 0.08, 0.10, 0.15\} [1/\text{h}]$, and for $r_{det} = r_{det2}$ the values of detachment coefficient were equal to $k_{det} = \{60, 80, 100, 150\} [1/(m \cdot h)]$

Figures 8 and 9 represent substrate concentration at the base of the biofilm for varying values of substrate concentrations in the liquid phase and detachment coefficients. Surprisingly, in both cases it was observed that with the increase of substrate concentration in the liquid phase, the values of concentration at the base of the biofilm become lower. It can be explained by the fact that thicker biofilms inevitably must contain more layers of microorganisms, which use more substrate, and also that as the structure thickens, the diffusional resistance is bigger. Additionally, simulations with lower detachment coefficient values resulted in lower substrate concentration at the base of the biofilm, because of the same reasons.

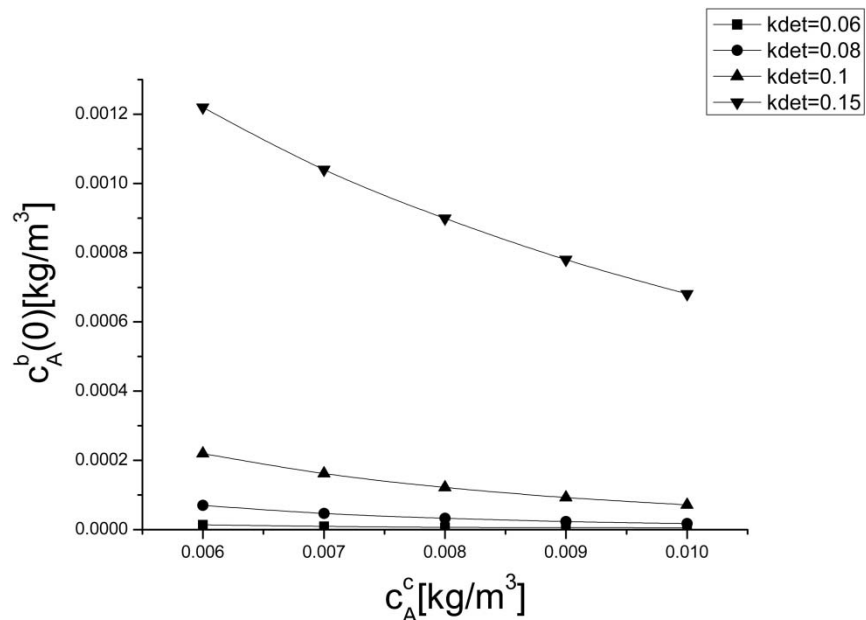


Fig. 8. Substrate concentration at the base of biofilm as a function of substrate concentration in liquid phase for varying values of detachment coefficient with r_{det1} detachment kinetics

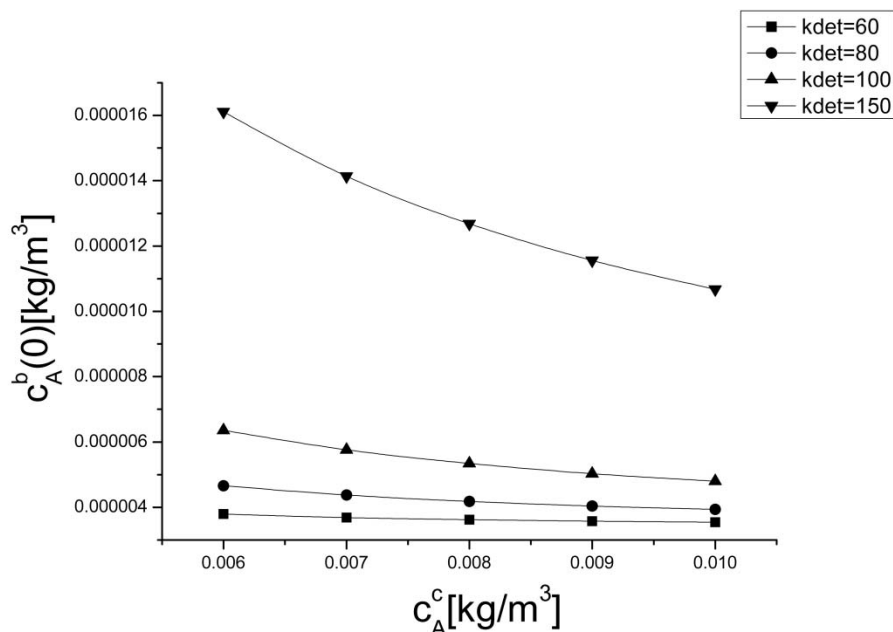


Fig. 9. Substrate concentration at the base of biofilm as a function of substrate concentration in liquid phase for varying values of detachment coefficient with r_{det2} detachment kinetics

In Figures 10 and 11 analogous relations for live cells concentrations were shown. Like in the case of substrate concentrations, the values get lower with the decrease of detachment coefficient and substrate

concentration values, which was expected, due to the need of substrate for the microorganisms' proliferation. However, while for the substrate concentration the biggest drop was observed for the highest considered detachment coefficient, in the case of the live cells concentration the greatest changes correspond to the slowest biofilm detachment.

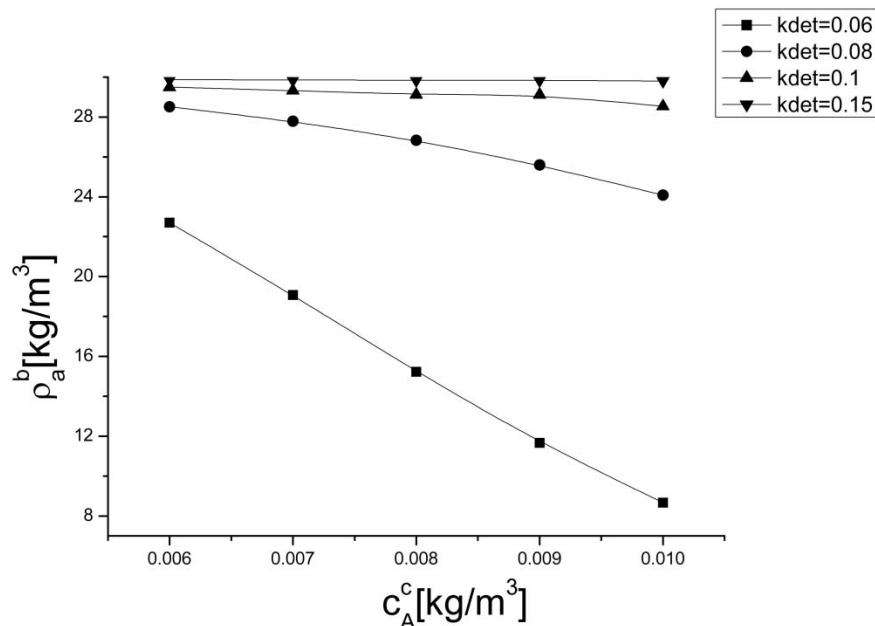


Fig. 10. Live cells concentration at the base of biofilm as a function of substrate concentration in liquid phase for varying values of detachment coefficient with r_{det1} detachment kinetics

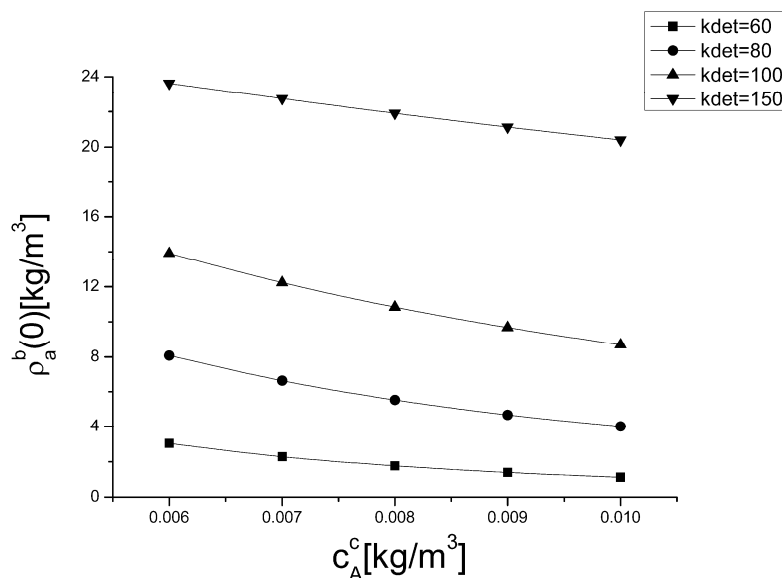


Fig. 11. Live cells concentration at the base of biofilm as a function of substrate concentration in liquid phase for varying values of detachment coefficient with r_{det2} detachment kinetics

As was already mentioned, the results of growth rate at the edge of the biofilm can be assumed to depend only on the concentration of substrate in that spot, which is connected to the third-type boundary condition, because the ratio of concentration of active cells to total cell concentration can be rounded up to one. Therefore, the curves representing biofilm growth rate as a function of liquid phase substrate concentration are almost identical, regardless of biofilm detachment rate constant values, as can be seen in Figures 12 and 13.

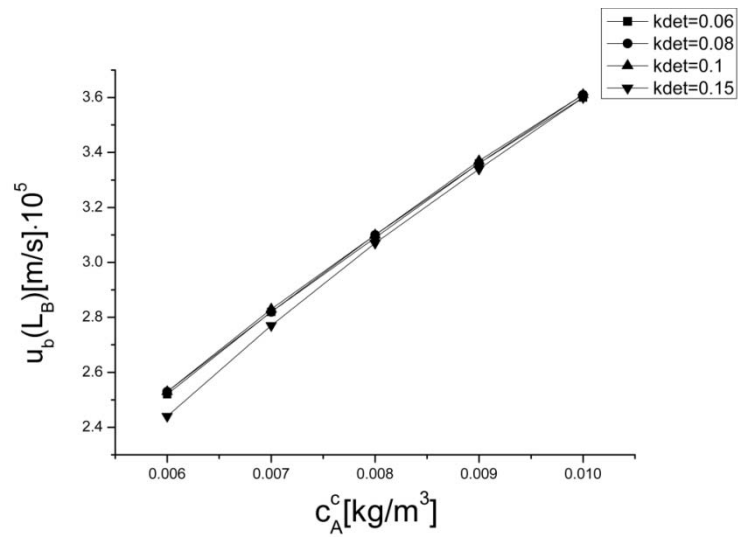


Fig. 12. Growth speed at the edge of biofilm as a function of substrate concentration in liquid phase for varying values of detachment coefficient with r_{det1} detachment kinetics

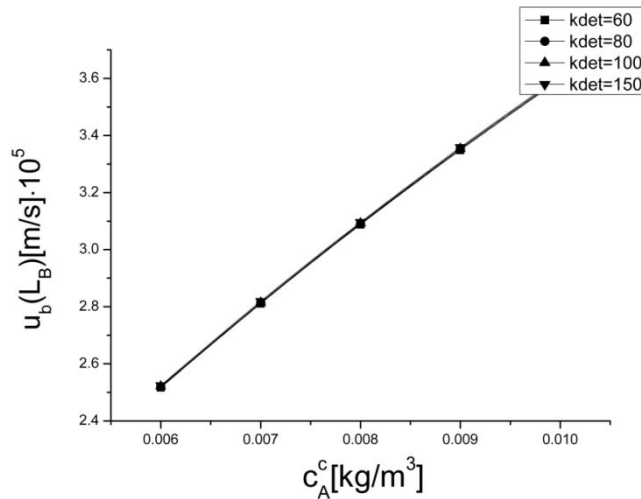


Fig. 13. Growth speed at the edge of biofilm as a function of substrate concentration in liquid phase for varying values of detachment coefficient with r_{det2} detachment kinetics

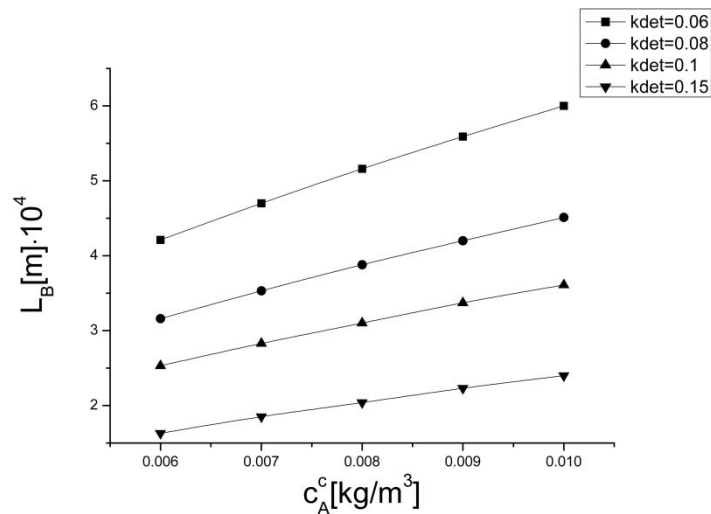


Fig. 14. Biofilm thickness as a function of substrate concentration in liquid phase for varying values of detachment coefficient with r_{det1} detachment kinetics

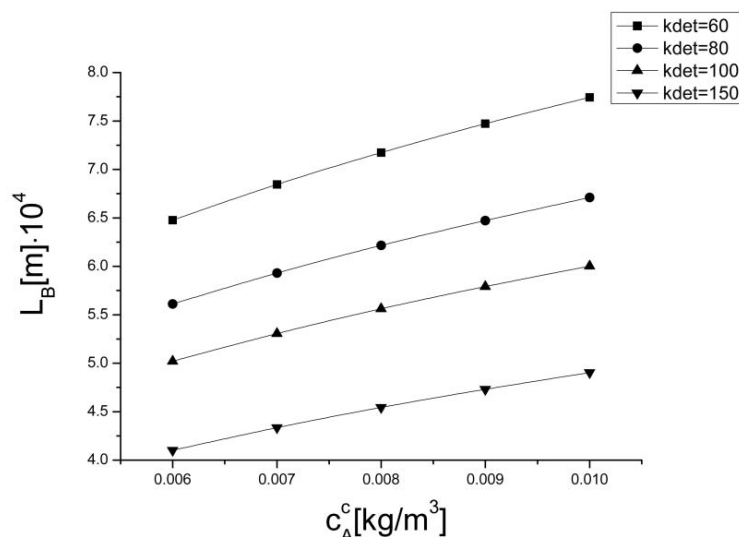


Fig. 15. Biofilm thickness as a function of substrate concentration in liquid phase for varying values of detachment coefficient with r_{det2} detachment kinetics

The curves in Figures 14 and 15 show that, regardless of the assumed detachment models, both the liquid phase substrate concentration and the detachment rate coefficient significantly affect the biofilm thickness. Obviously, higher substrate concentrations in the liquid phase and lower biofilm detachment coefficients resulted in higher values of biofilm thickness. In all cases the figures show that the functions $L_B = f(C_A^c)$ are close to linear, which makes them easy for potential extrapolation

3.3. Death rate coefficient influence on active cell distribution

A set of simulations for different values of death rate coefficient was performed to see how it affects biofilm behaviour. The biofilm detachment kinetics used in this case was proportional to the biofilm thickness squared. The detachment coefficient was equal to $k_{det} = 100$ [1/mh], and the concentration of carbon substrate in the liquid phase was equal $c_A^c = 0.08$ [kg/m³]. The assumed death rate coefficient values were equal to $k_o = \{3 \cdot 10^{-4}, 4 \cdot 10^{-4}, 5 \cdot 10^{-4}, 6 \cdot 10^{-4}\}$ [1/h].

The results of calculated biofilm thickness values are presented in Table 3. It shows that the change of cell death rate has a very small effect on the biofilm thickness. However, as can be seen in Figure 16, the influence on active cell distribution throughout the biofilm is significant. Although near the edge of the biofilm the curves are close to each other, the closer to the base of biofilm, the difference between active cells concentration values becomes more distinct, and with the increase of the death rate coefficient live cells concentrations become smaller.

Table 3. Biofilm thickness for varying values of death rate coefficient with r_{det2} detachment kinetics

k_o [1/h]	L_b [m]
3.00E-03	5.564E-04
4.00E-03	5.561E-04
5.00E-03	5.559E-04
6.00E-03	5.556E-04

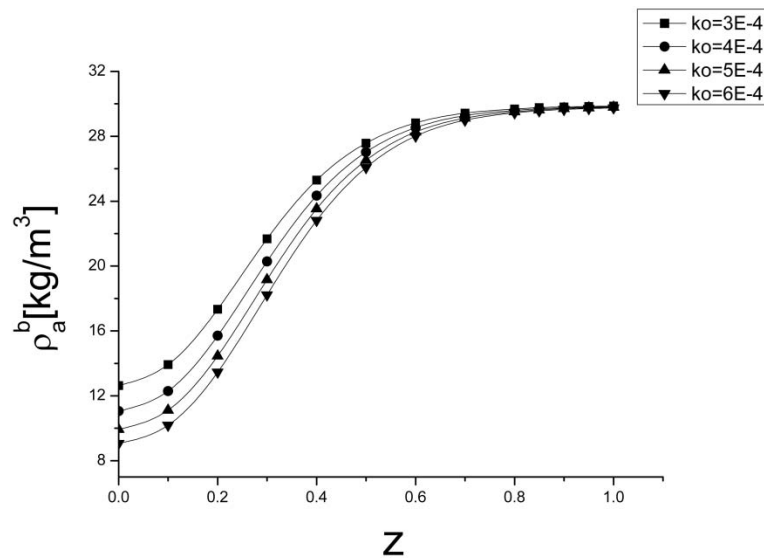


Fig. 16. Distribution of live cells as a function of the dimensionless variable z for varying values of death rate coefficient with r_{det2} detachment kinetics

4. CONCLUSIONS

The output data of the created program, containing information about distribution of carbon substrate and biologically active cells and biofilm growth rate in specified points, was used to examine certain aspects of biofilms' behaviour.

One can conclude that a change of the assumed biofilm detachment model affects not only the thickness of the biofilm, but also other variables including live cells distribution throughout the biofilm. The results of simulations have shown that adding more substrate to the liquid phase does not have a positive effect on microorganisms' access to the substrate at the base of the biofilm, which is caused by the fact that the biofilm thickness reaches larger values and that the diffusional resistance of the biofilm becomes higher. It was also proven that biofilm detachment rate has a significant effect on its thickness.

By performing simulations with varying death rate coefficient it was shown that although the biofilm thickness variations were negligible, the active cells concentrations at specific points were significantly different.

The authors would like to thank Szymon Skoneczny for his contribution in the creation of the program for numeric simulations. Michał Blatkiewicz would also like to thank for the financial support provided by the Rector's Scholarship for PhD students.

SYMBOLS

c_A	substrate concentration, kg/m^3
D_e	diffusion coefficient, m^2/h
k_{det}	biofilm detachment coefficient, $1/\text{h}$ or $1/\text{mh}$
k_o	cell death rate constant, $1/\text{h}$
k_s	mass penetration coefficient, m^2/h^2
K_s	Monod coefficient, kg/m^3

L_b	biofilm thickness, m
r	reaction rate, $\text{kg/m}^3\text{h}$
S	external biofilm surface, m^2
t	time, h
u_b	linear speed of biofilm growth, m/h
w	yield coefficient, -
x	length variable in biofilm, m
z	dimensionless length variable in biofilm, -

Greek symbols

μ_{\max}	maximum biomass growth coefficient, 1/h
ρ_a	active cells concentration, kg/m^3
ρ_b	total cell concentration, kg/m^3
ρ_i	dead cell concentration, kg/m^3

Superscripts

b	biofilm phase
c	liquid phase

Subscripts

A	substrate
B	biomass

REFERENCES

- Bryers J.D., 1988. *Modeling biofilm accumulation*, In: *Physiological models in microbiology*, 2, CRC Press, 109–144.
- Hsien T.-Y., Lin Y.-H., 2005. Biodegradation of phenolic wastewater in a fixed biofilm reactor. *Biochem Eng. J.*, 27, 95-103. DOI: 10.1016/j.bej.2005.08.023.
- Janssens J.C A., Steenackers H., Robijns S., Gellens E., Levin J., Zhao H., Hermans K., De Coster D., Verhoeven T.L., Marchal K., Vanderleyden J., De Vos D.E., De Keersmaecker S.C.J., 2008. Brominated furanones inhibit biofilm formation by *Salmonella enterica* serovar typhimurium, *App. Environ. Microbiol.*, 74, 6639-6648. DOI: 10.1128/AEM.01262-08.
- Kommedal R., Bakke R., 2003. *Modeling Pseudomonas Aeruginosa Biofilm Detachment*. HiT Working Paper, Telemark University College, 3/2003, 1-29.
- Lapidou C.S., Aravas N., 2007. Variation in the mechanical properties of a porous multi-phase biofilm under compression due to void closure. *Water Sci. Technol.*, 55, 447-453. DOI: 10.2166/wst.2007.289.
- Liao Q., Wang Y., Wang Y., Chen R., Zhu X., Pu Y., Lee D., 2012. Two-dimension mathematical modeling of photosynthetic bacterial biofilm growth and formation. *Int. J. Hydrog. Energy*, 37, 15607-15615. DOI: 10.1016/j.ijhydene.2012.03.056.
- Liu S., Horn H., 2011. Effects of biofilm geometry on deammonification biofilm performance: A simulation study. *Bioresour. Technol.*, 116, 252-258. DOI: 10.1016/j.biortech.2011.12.131.
- Paul E., Ochoa J.C., Pechaud Y., Liu Y., Line A., 2012. Effect of shear stress and growth conditions on detachment and physical properties of biofilms. *Water Res.*, 46, 5499-5508. DOI: 10.1016/j.watres.2012.07.029.
- Peyton B.M., Characklis W.G., 1992. Kinetics of biofilm detachment. *Water Sci. Technol.*, 26, 1995-1998.
- Sidhu M.S., Langsrud S., Holck A., 2001. Disinfectant and antibiotic resistance of lactic acid bacteria isolated from the food industry. *Microb. Drug Resist.*, 7, 73-83. DOI: 10.1089/107662901750152846.

- Srey S., Iqbal K., Jahid K., Ha S., 2012. Biofilm formation in food industries: A food safety concern. *Food Control*, 31, 572-585. DOI: 10.1016/j.foodcont.2012.12.001.
- Stewart P., Hamilton M., Goldstein B., Schneider B., 1996. Modeling biocide action against biofilms. *Biotech. Bioeng.*, 49, 445-455. DOI: 10.1002/(SICI)1097-0290(19960220)49:4<445::AID-BIT12>3.0.CO;2-9.
- Stoodley P., Sauer K., Davies D.G., Costerton J.W., 2002. Biofilms as complex differentiated communities. *Annual Rev. Microbiol.*, 56, 187-209. DOI: 10.1146/annurev.micro.56.012302.160705.
- Topiwala H., Hamer G., 1971. Effect of wall growth in steady-state continuous cultures. *Biotech. Bioeng.*, 13, 919-922. DOI: 10.1002/bit.260130614.
- Wanner O., Gujer W., 1985. A multispecies biofilm model. *Water Sci. Technol.*, 26, 314-328. DOI: 10.1002/bit.260280304.

Received 21 March 2013

Received in revised form 26 September 2013

Accepted 10 October 2013